the γ hydride, however, expansion takes place mainly in the a parameter. Interpretation of these interesting structural differences must await neutron diffraction measurements on the RCo_3 hydrides.

As noted above, the RFe_3 compounds form only two hydrides—the α or terminal phases and a second hydride. It is not entirely clear whether this should be designated β or γ. We incline to regard it as the γ hydride, by analogy with the crystallographic behavior of the RCo_3–H systems, since it involves an expansion in both the a and c parameters.

The H_2 pressures over the RFe_3–H systems are consistently lower than those of the RCo_3–H system in the two-phase regions. However, the RFe_3 phase absorbs less hydrogen at the maximum pressure utilized (400 psig) than the corresponding RCo_3 compound. Clearly, the γ RFe_3–H phase is stabler against hydrogen loss than the γ RCo_3–H phase at the hydrogen-poor end of the range of stability of the phase, and this order of stability exists for all hydrogen concentrations in the α phases.

There are then three classes of systematic behavior exhibited by the RT_x–H systems with regard to affinity for hydrogen: 1, a decrease as the atomic number of R increases; 2, a decrease as x increases; 3, a decrease when Fe is replaced by Co. In each of these three cases the decrease in affinity for hydrogen accompanies a change in chemical composition of stoichiometry which leads to a decrease in lattice size. We shall return to this point below.

Several absorption experiments were made to investigate the extent of the hysteresis between absorption and desorption of hydrogen for the 1:3 compounds. The behavior was found to be similar to that of the 1:5 cobalt compounds[7] in that the quantity $\Delta P/P$ at different temperatures for the same hydride was essentially constant. ΔP is the difference in plateau pressure observed in the absorption and desorption experiments. In most treatments of the hysteresis phenomenon the lattice expansion and the degree of hysteresis are interrelated.[8] In the 1:3 cobalt case where two hydrides are formed, the value of $\Delta P/P$ was greater for the γ hydride than for the β hydride. This is as expected since the lattice expansion is greater for the γ hydride.

The main difference in hydrogen absorption of the 1:3 cobalt or iron phases and that of the RT_5 compounds is the temperature at which desorption of hydrogen takes place above atmospheric pressure. The $LaNi_5$ desorption pressure at room temperature is 2.5 atm. For $LaCo_5$ a temperature of 90 °C is required to generate a hydrogen pressure exceeding 1 atm. The corresponding temperatures are 180 and 215 °C for the RCo_3 and RFe_3 phases, respectively. The RT_3 compounds thus afford a low-pressure hydrogen storage and delivery system which can easily be controlled by temperature.

Above, it was pointed out that in the RT_x phase the affinity for hydrogen is reduced by increasing the atomic number of R or T or by increasing x; all of these result in a more compact lattice. The work of Kuijpers and Loopstra[9] shows that molecular H_2 (or more exactly D_2) in $PrCo_5$ is broken down into the monatomic form and the atoms reside in certain interstitial sites. As the lattice size is diminished, the volume of the interstitial site decreases correspondingly. Superficially one might ascribe the systematics noted to the varying size of the site in which the H is occupied. We doubt that matters are that simple since the size of H^+, the species which probably most nearly resembles the dissolved form of hydrogen, is far smaller than that of the interstice. Probably the variations noted affect the band structure in these materials in a systematic way, and it is this which leads to the observed systematic trends noted in the hydrogen affinity of the RT_x phases. APW band calculations on selected RT_x phases are being carried out in this laboratory, and these may in time be useful in elucidating the receptivity of these phases for hydrogen.

Acknowledgment. This work was assisted by a contract with the Energy Research and Development Administration.

Registry No. $GdCo_3$, 12017-50-4; $TbCo_3$, 12187-47-2; $DyCo_3$, 12187-40-5; $HoCo_3$, 12140-00-0; $ErCo_3$, 12134-04-2; $GdFe_3$, 12023-46-0; $TbFe_3$, 12268-62-1; $DyFe_3$, 12517-72-5; $HoFe_3$, 12361-81-8; $ErFe_3$, 12400-78-1; H_2, 1333-74-0.

References and Notes

(1) J. H. N. van Vucht, F. A. Kuijpers, and H. C. A. M. Bruning, *Philips Res. Rep.*, **25**, 133 (1970).
(2) F. A. Kuijpers, *J. Less-Common Met.*, **27**, 27 (1972).
(3) T. Takeshita, W. E. Wallace, and R. S. Craig, *Inorg. Chem.*, **13**, 2282, 2283 (1974).
(4) K. H. J. Buschow and H. V. Van Mal, *J. Less-Common Met.*, **29**, 203 (1972).
(5) R. Lemaire and D. Paccard, *Bull. Soc. Fr. Mineral. Cristallogr.*, **92**, 9 (1969).
(6) F. A. Kuijpers, Ph.D. Thesis, Technische Hogeschool, Delft, 1973.
(7) F. A. Kuijpers and H. H. Van Mal, *J. Less-Common Met.*, **23**, 395 (1971).
(8) See, for example, N. A. Scholtus, and W. K. Hall, *J. Chem. Phys.*, **39**, 868 (1963).
(9) F. A. Kuijpers and B. D. Loopstra, *J. Phys. (Paris) Colloq.*, **32**, C1-657 (1971).

Contribution from The Technical University of Denmark, Chemistry Department A, DK-2800 Lyngby, Denmark

Lower Oxidation States of Tellurium. 4. Tetratellurium(2+), Hexatellurium(2+), and Octatellurium(2+) in Chloroaluminate Melts

R. FEHRMANN, N. J. BJERRUM,* and H. A. ANDREASEN

Received January 15, 1976 AIC60040L

The solvated entities Te_4^{2+}, Te_6^{2+}, and Te_8^{2+} have been identified in reaction mixtures of dilute solutions of $TeCl_4$ and elementary tellurium by a combination of a spectrophotometric and a potentiometric method. The spectra of the individual tellurium species in the low-melting NaCl–$AlCl_3$ (37:63 mol %) solvent at 250 °C are calculated from the spectra of the experimental mixtures. pK values (based on molar concentrations) for the reactions $2Te^{4+}(soln) + 7Te_6^{2+}(soln) \rightleftarrows 11Te_4^{2+}(soln)$ and $Te_4^{2+}(soln) + Te_8^{2+}(soln) \rightleftarrows 2Te_6^{2+}(soln)$ were found by both methods. The spectrophotometric method (at 250 °C) gave for the two reactions pK values of −12 and −0.4 with nonlinear confidence limits (95%) of $-\infty$ to −9 and −2.2 to −0.2, respectively. The potentiometric method (at 150 °C) gave for the two reactions pK values of −17 and −0.93 with nonlinear confidence limits (95%) of $-\infty$ to −10 and −1.03 to −0.84, respectively.

Introduction

Previously[1] it has been mentioned that in an NaCl–$AlCl_3$ (37:63 mol %) melt three low oxidation states of tellurium seem to be formed, when Te(IV) is reduced with tellurium. One of these species has been shown[1] to be Te_4^{2+}, whereas the other species have only been suggested to be Te_6^{2+} and Te_8^{2+}.[2] In

the present paper evidence is given for these species in chloroaluminate melts. The observation of two of these three species is in agreement with work by Corbett and co-workers.[3] In this work it was shown that tellurium compounds with oxidation states $+^1/_2$ and $+^1/_3$ exist. The $+^1/_2$ oxidation state was later shown to contain the Te_4^{2+} entity in the form of $Te_4(AlCl_4)_2$ or $Te_4(Al_2Cl_7)_2$,[4] but no x-ray structure has been given for the $+^1/_3$ oxidation state. Tellurium species in the oxidation states $+^1/_2$ and $+^1/_3$ have been found in other highly acidic media.[5]

Experimental Section

Materials and Measurements. The materials used in the present work are purified or made in the same way as in previous work.[1,6] An analysis of the $TeCl_4$ used gave as an average of four measurements a chlorine content of 52.73 ± 0.11% (the theoretical values for $TeCl_4$ is 52.64%). The experimental technique was the same as in previous work.[1,7,8] The same type of electrochemical cells with inert electrodes of vitreous carbon were used, but N_2 gas was added to the cells instead of Cl_2 gas. In all potentiometric measurements the pressure was the same over the melts in the two cell compartments. The measured potentials were found constant within ca. ±0.01 mV (over a period of several hours), when equilibrium conditions were reached.

Methods of Investigation

General Considerations. The initial molar amount of one of the added substances (in the present work NaCl, $AlCl_3$, $TeCl_4$, and Te) dissolved in 1 l. of the melt is defined as its formality. The ratio between two formalities is called the formality ratio for these substances and is denoted by the letter R. The densities of the solutions were calculated assuming ideal mixtures of Te, $TeCl_4$, and NaCl–$AlCl_3$. This assumption will only give rise to a small error as the amounts of Te and $TeCl_4$ added were small compared with the amounts of NaCl–$AlCl_3$. The densities of Te, $TeCl_4$, and NaCl–$AlCl_3$ were obtained from the work of Damiens,[9] Simons,[10] and Boston,[11] respectively. Due to the reaction $Al_2Cl_7^- + Cl^- \rightleftarrows 2AlCl_4^-$ [12] the melt was well buffered with respect to the chloride activity.

Spectra. The formal absorptivity is defined by $A(lc')^{-1}$, where A is the absorbance corrected for the absorbance of cell and solvent, l is the path length, and c' is the formality. In the present work all of the measured absorptivities have been divided by the total concentration of tellurium. This is expressed in the formulation $A/lc'_{Te,total}$, where A and l have the meanings given above and $c'_{Te,total}$ is the total concentration of tellurium.

It has previously been mentioned[14] that it can be shown from the Bouguer–Beer law, the law of additive absorbances, and the mass action relation that straight lines on a plot of the formal absorptivity vs. the formality ratio (for example of Te:$TeCl_4$) can only be obtained for a system with two species; that this is so can be seen from the following arguments. From the Bouguer–Beer law and the law of additive absorbance one obtains the equation

$$A(\nu'_1)/c'_{Te(IV)}l = \epsilon_1(\nu'_1)c_1/c'_{Te(IV)} + \epsilon_2(\nu'_1)c_2/c'_{Te(IV)} + \epsilon_3(\nu'_1)c_3/c'_{Te(IV)} + \ldots + \epsilon_n(\nu'_1)c_n/c'_{Te(IV)} \quad (1)$$

where $A(\nu'_1)$ is the total absorptivity at the wavenumber ν'_1, $c'_{Te(IV)}$ is the formal concentration of Te(IV), $\epsilon_1(\nu'_1)$ is the molar absorptivity of the first species and c_1 is the concentration of the first species. The formality ratio, R, can be expressed as

$$R = f_1c_1/c'_{Te(IV)} + f_2c_2/c'_{Te(IV)} + f_3c_3/c'_{Te(IV)} + \ldots + f_nc_n/c'_{Te(IV)} \quad (2)$$

where f_1 is the stoichiometric amount of tellurium in the first species coming from the added tellurium. The formal charge of Te(IV) (i.e., 4+) can be expressed as

$$Z = P_1c_1/c'_{Te(IV)} + P_2c_2/c'_{Te(IV)} + P_3c_3/c'_{Te(IV)} + \ldots + P_nc_n/c'_{Te(IV)} \quad (3)$$

where Z is the formal charge of Te(IV) and p_1 is the stoichiometric amount of tellurium in the first species coming from the added $TeCl_4$ times the formal charge of Te(IV). From the law of mass action one obtains

$$K_1 = c_1^{l_{1,1}}\ c_2^{l_{1,2}}\ c_3^{l_{1,3}} \quad (4)$$

$$K_2 = c_2^{l_{2,2}}\ c_3^{l_{2,3}}\ c_4^{l_{2,4}} \quad (5)$$

$$\vdots$$

$$K_{n-2} = c_{n-2}^{l_{n-2,n-2}}\ c_{n-1}^{l_{n-2,n-1}}\ c_n^{l_{n-2,n}} \quad (6)$$

where K_1 is the equilibrium constant for the first equilibrium and $|l_{1,1}|$ is the reaction coefficient for the first species in the first equilibrium. From these equations (which are irreducible) the concentrations of all species up to the nth species can always be calculated from c_1 and c_2 and all the equilibrium constants from K_1 to K_{n-2}. The concentrations of all of these species can now be introduced into eq 1–3. If we first look at a two-species system, eq 1–3 will contain only two terms with $c_1/c'_{Te(IV)}$ and $c_2/c'_{Te(IV)}$ as parameters. Equations 1–3 can be solved by elimination and we will obtain an equation of the form

$$a_1A(\nu')/c'_{Te(IV)}l + a_2R + a_3Z = 0 \quad (7)$$

where a_1, a_2, and a_3 are constants. Since Z is also constant, it is obvious that we have a linear relationship between $A(\nu')/c'_{Te(IV)}l$ and R. The important thing is now that if we deal with a system with more than two species, nonlinear terms will be introduced into eq 1–3. An elimination of the parameters which are now c_1 and c_2 (since it is normally not possible under these circumstance to use $c_1/c'_{Te(IV)}$ and $c_2/c'_{Te(IV)}$ as parameters) will give us a nonlinear equation between $A(\nu')/c'_{Te(IV)}l$, R, and $c'_{Te(IV)}$ (i.e., curved lines at constant $c'_{Te(IV)}$). In practice it can of course be difficult to distinguish between slightly curved lines and straight lines. By varying the formality of $TeCl_4$ the relative concentrations of the different species will, if there are more than two, normally be changed due to the law of mass action, and this will again affect the formal absorptivity. Therefore, by varying the formality of the highest oxidation state (in the present case $TeCl_4$) one can identify cases where it is difficult to distinguish between a straight line and a slightly curved line. Finally it is also important to make plots at more than one wavenumber.

It can also be shown[13,14] from the Bouguer–Beer law and the law of additive absorbances that if we deal with different spectra obtained at different compositions, a general equation involving three matrices can be put forward, i.e.

$$[l_mc_{mi}][\epsilon_i(\nu'_n)] = [A_m(\nu'_n)] \quad (8)$$

where l_m is the path length at the mth composition, c_{mi} is the concentration of the ith species for the mth composition, $\epsilon_i(\nu'_n)$ is the molar absorptivity of the ith species at the wavenumber ν'_n, and $A_m(\nu'_n)$ is the total absorbance of the mth composition at the wavenumber ν'_n. From the model put forward to explain the spectral changes of the melt and from an arbitrarily chosen equilibrium constant, the concentration of each species c_i can be calculated. This (together with the measured absorbances at different wavenumbers and different compositions) is now introduced in eq 8 and the "best" values of $\epsilon_i(\nu'_n)$ (least squares) are calculated. By varying systematically the

equilibrium constant, the deviation (least squares) between the measured and calculated spectra can be minimized. This procedure can be applied to any equilibrium and the results can be used in a model discrimination.

In all calculations regarding the spectrophotometric work the variation in the activity coefficients was neglected. This can be justified by the fact that the ionic strength of the solvent was high and the concentrations of the solute species were low (less than 0.015 M).

Cell Potentials. Previously[7,8] we have used an electrode cell made of Pyrex with vitreous carbon from Carbone-Lorraine fused into the bottom for chlorine–chloride electrode measurements. The same cell can be used for measurements with the different tellurium species. If we look at one redox pair which we generally will call Te_q^{r+} and Te_v^{x+} (r, q, v, and x are integers), the composition of the cell can be given as

$$\text{carbon I}\left|\begin{array}{l}\text{solution I}\\ Te_q^{r+}\text{ and }Te_v^{x+}\\ \text{in NaCl–AlCl}_3\\ (37{:}63\text{ mol \%})\end{array}\right|\text{porous pin}\left|\begin{array}{l}\text{solution II}\\ Te_q^{r+}\text{ and }Te_v^{x+}\\ \text{in NaCl–AlCl}_3\\ (37{:}63\text{ mol \%})\end{array}\right|\text{carbon II} \quad (9)$$

At each electrode we have the equilibrium

$$qTe_v^{x+} \rightleftarrows vTe_q^{r+} + ne^- \quad (10)$$

or

$$(q/n)Te_v^{x+} \rightleftarrows (v/n)Te_q^{r+} + e^- \quad (11)$$

where e^- is the electron and n is the number of electrons. The potential of the cell can now generally[15] be given as

$$\Delta E = \frac{1}{F}\int_I^{II}\Sigma_i t_i(-z_i^{-1}\,d\mu_i + n^{-1}v\,d\mu_{Te_q^{r+}} - n^{-1}q\,d\mu_{Te_v^{x+}} \quad (12)$$

where t_i, z_i, and μ_i are the transference number, charge, and chemical potential for the ith ion, respectively. From measurements on the NaCl–$AlCl_3$[12] systems it is reasonable to assume that the ions present in the cell compartments from the solvent are Na^+, $Al_2Cl_7^-$, and $AlCl_4^-$. Since we, in the calculations regarding the potentiometric measurements, will restrict ourselves to Te:$TeCl_4$ formality ratio ranges where two or three different tellurium species are present, the tellurium species can be given as Te_q^{r+}, Te_v^{x+}, and Te_y^{z+} (z and y are integers). Under these circumstances eq 12 can be expressed in activities

$$\Delta E = \frac{RT}{F}\int_I^{II} n^{-1}v\,d\ln[Te_q^{r+}] - n^{-1}q\,d\ln[Te_v^{x+}] - t_{Na^+}\,d\ln[Na^+] + t_{Al_2Cl_7^-}\,d\ln[Al_2Cl_7^-] + t_{AlCl_4^-}\,d\ln[AlCl_4^-] - \frac{1}{r}t_{Teq^{r+}}\,d\ln[Te_q^{r+}] - \frac{1}{x}t_{Te_v^{x+}}\,d\ln[Te_v^{x+}] - \frac{1}{z}t_{Te_y^{z+}}\,d\ln[Te_y^{z+}] \quad (13)$$

Unfortunately no data are available for the transference numbers in this equation, but since the solvent is the same in both electrode compartments, it is reasonable to neglect variations with compositions in the transference number for Na^+, $Al_2Cl_7^-$, and $AlCl_4^-$. The concentrations of Te_q^{r+}, Te_v^{x+}, and Te_y^{z+} are by comparison rather small and vary a great deal. A reasonable assumption here is that the transference number is proportional to the concentration and hence the activity of each species. This can be expressed by

$$\Delta E = \frac{RT}{F}\int_I^{II} n^{-1}v\,d\ln[Te_q^{r+}] - n^{-1}q\,d\ln[Te_v^{x+}] - t^0_{Na^+}\,d\ln[Na^+] + t^0_{Al_2Cl_7^-}\,d\ln[Al_2Cl_7^-] + t^0_{AlCl_4^-}\,d\ln[AlCl_4^-] - \frac{1}{r}k_{Teq^{r+}}[Te_q^{r+}]\,d\ln[Te_q^{r+}] - \frac{1}{x}k_{Te_v^{x+}}[Te_v^{x+}]\,d\ln[Te_v^{x+}] - \frac{1}{z}k_{Te_y^{z+}}[Te_y^{z+}]\,d\ln[Te_y^{z+}] \quad (14)$$

where $t^0_{Na^+}$, $t^0_{Al_2Cl_7^-}$, and $t^0_{AlCl_4^-}$ are the transference numbers in pure NaCl–$AlCl_3$ (37:63 mol %) and $k_{Teq^{r+}}$, $k_{Te_v^{x+}}$, and $k_{Te_y^{z+}}$ are constants, which multiplied by the concentrations of the respective species give the transference numbers for the same species. An integration of this expression gives

$$\Delta E = \frac{RT}{F}\ln\frac{[Te_q^{r+}]_{II}^{n^{-1}v}[Te_v^{x+}]_I^{n^{-1}q}}{[Te_q^{r+}]_I^{n^{-1}v}[Te_v^{x+}]_{II}^{n^{-1}q}} - \frac{RT}{F}t^0_{Na^+}\ln\frac{[Na^+]_{II}}{[Na^+]_I} + \frac{RT}{F}t^0_{Al_2Cl_7^-}\ln\frac{[Al_2Cl_7^-]_{II}}{[Al_2Cl_7^-]_I} + \frac{RT}{F}t^0_{AlCl_4^-}\ln\frac{[AlCl_4^-]_{II}}{[AlCl_4^-]_I} - \frac{RT}{F}\frac{k_{Teq^{r+}}}{r}([Te_q^{r+}]_{II} - [Te_q^{r+}]_I) - \frac{RT}{F}\frac{k_{Te_v^{x+}}}{x}([Te_v^{x+}]_{II} - [Te_v^{x+}]_I) - \frac{RT}{F}\frac{k_{Te_y^{z+}}}{z}([Te_y^{z+}]_{II} - [Te_y^{z+}]_I) \quad (15)$$

The values of $t^0_{Na^+}$, $t^0_{Al_2Cl_7^-}$, $t^0_{AlCl_4^-}$, $k_{Teq^{r+}}$, $k_{Te_v^{x+}}$, and $k_{Te_y^{z+}}$ are not known, but if we assume that the mobilities are independent of the charges on the ions and are inversely proportional to their ionic radii, we can get an idea about the sizes of the last six terms in eq 15. These terms will under all circumstances be small. The assumption that the mobilities are approximately independent of the charge on the ions seems to be correct for dilute solutions in water,[16] whereas the mobility seems to decrease with increasing formal charge for molten salt solution[17] (perhaps due to complex formation). The first assumption, however, will give larger contributions to the last three terms and will therefore be chosen as the worst case. The assumption that the mobility is inversely proportional to the ionic radius seems to fit reasonably well for a number of molten salts, where the anions and cations are well defined.[17]

The variation in the activity coefficients has been neglected in the potentiometric work. Due to lack of data it is impossible to make an exact calculation of this change. However, since the solvent, which has a high ionic strength, is the same in both cell compartments and the concentration of solute species is in the range 0.09–0.18 M, it is reasonable to expect the variation in activity coefficients to be small. An idea about the variation in activity coefficients for solute species in chloroaluminate melts can be obtained from potentiometric measurements on the KCl–$KAlCl_4$ system.[18] If we assume that the found deviation from ideality for the chloride ions in this system is due to changes in the activity coefficient, a relative change of $-2 \pm 5\%$ (standard error) is obtained in going from a ca. 0.34 M to a 0.56 M solution of KCl in $KAlCl_4$ at 300 °C.

Results and Discussion

Spectrophotometric Study of Tellurium Species Formed in the NaCl–$AlCl_3$ (37:63 mol %) Melt. Three tellurium species are known to appear successively in acidic NaCl–$AlCl_3$ melts by reductic ı of Te(IV) with tellurium. Previously these species

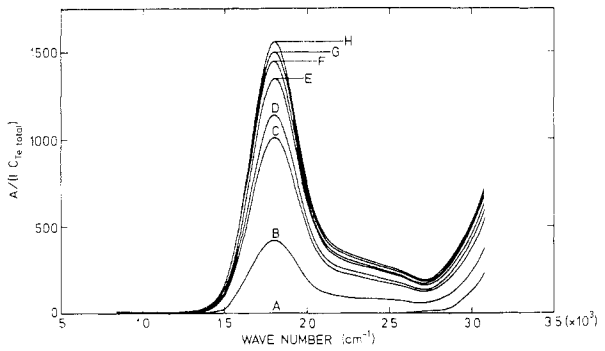

Figure 1. Series of spectra of solutions of $TeCl_4$ reduced with tellurium. Te:$TeCl_4$ formality ratio and formality of $TeCl_4$: A, 0.00_0, 0.006 96; B, 0.29_7, 0.006 96; C, 1.26_1, 0.006 96; D, 1.71_9, 0.006 96; E, 2.79_1, 0.006 96; F, 3.89_3, 0.006 96; G, 5.22_0, 0.005 39; H, 6.60_7, 0.006 96. Solvent is NaCl–$AlCl_3$ (37:63 mol %) at 250 °C.

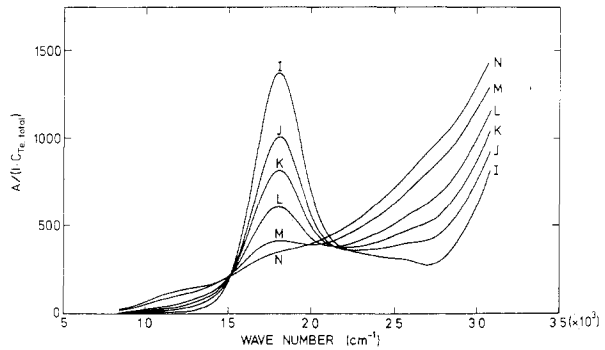

Figure 2. Series of spectra of solutions of $TeCl_4$ reduced with tellurium. Te:$TeCl_4$ formality ratio and formality of $TeCl_4$: I, 7.48_9, 0.005 39; J, 8.45_8, 0.005 39; K, 9.18_3, 0.005 39; L, 10.21_2, 0.005 39; M, 12.02_0, 0.005 38; N, 13.59_1, 0.005 38.

have for convenience been labeled I, II, and III.[1] Since it is important for the present work, the spectra from the previous publication (plus some hitherto unpublished spectra) will be given in a new form and discussed again. The measured spectra are conveniently divided into two ranges determined by the formality ratio of Te:$TeCl_4$. In the formality ratio range 0–7 shown in Figure 1 only one species, Te_4^{2+} (previously labeled I), is formed by the reduction of $TeCl_4$ by tellurium. This can be verified by the observation that the Bouguer–Beer law with respect to the formality of tellurium was followed at all measured wavenumbers below 25×10^3 cm^{-1} and that changes in temperature over the range 130–310 °C produced only minor changes in the spectrum calculated on the basis of added tellurium. Below 25×10^3 cm^{-1} Te(IV) starts to absorb. Te(IV) is probably present as $TeCl_3^+$.[14,19] If the formality ratio Te:$TeCl_4$ is increased to values higher than 7, the peak at 18.0×10^3 cm^{-1} (due to Te_4^{2+}), begins to decrease. This is shown in Figure 2. As seen from Figure 2 the spectra marked I, J, and K seem to form two isosbestic points located at 15.2×10^3 and 22.0×10^3 cm^{-1}, whereas the spectra L, M, and N do not seem to form isosbestic points. A closer analysis of the spectra I, J, and K shows that these are internally linearly dependent. This suggests that apart from Te_4^{2+} only one new reaction product (previously labeled II) is present in this formality ratio range. For formality ratios from 10.2 to 13.6 the spectra indicate that the two-species equilibrium is no more present. What can be observed here is a decrease of the peak at 18.0×10^3 cm^{-1} (due to Te_4^{2+}) and the appearance of a shoulder at 11.5×10^3 cm^{-1} and a shoulder at 17.0×10^3 cm^{-1}. The shoulder at 17.0×10^3 cm^{-1} could be due to II, but the shoulder at 11.5×10^3 cm^{-1} must be due to another species (previously labeled III).

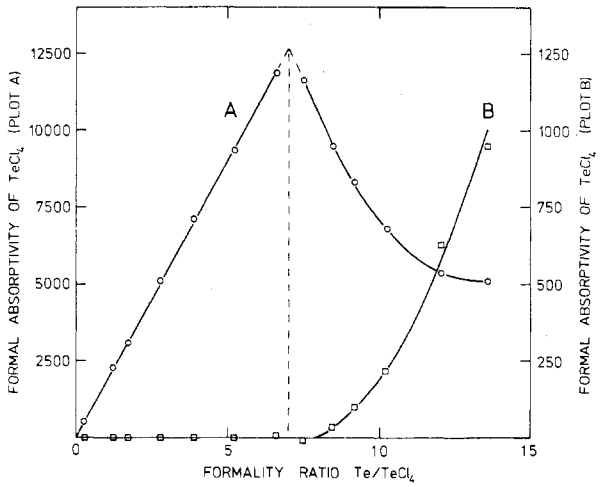

Figure 3. Relations between the formal absorptivity of $TeCl_4$ and the Te:$TeCl_4$ formality ratio measured at two different wavenumbers: A, circles at 18.0×10^3 cm^{-1}; B, squares at 10.0×10^3 cm^{-1}. Dashed line indicates formality ratio 7.

Another way to look at the results obtained is given in Figure 3. Here the formal absorptivities of $TeCl_4$ measured at two wavenumbers 10.0×10^3 and 18.0×10^3 cm^{-1} are plotted vs. the Te:$TeCl_4$ formality ratio. From the plot shown in Figure 3 it can be seen that there is a linear relationship between the formal absorptivity of $TeCl_4$ and the formality ratio in the range from 0 to 7 indicating a two-species system (i.e., $TeCl_3^+$ and Te_4^{2+}). In the range from 7 to 9 there seems, judged from the formal absorptivity at 18.0×10^3 cm^{-1}, to be another range with linear relationship. If we look at the formal absorptivity of $TeCl_4$ at 10.0×10^3 cm^{-1} (the shown plot is multiplied by 10 compared with the plot of the formal absorptivity measured at 18.0×10^3 cm^{-1}), it can be seen that III does not absorb in the range 7–8 but that it starts to absorb above 8. Therefore, in the range between 7 and 8 only two species (Te_4^{2+} and II) are present and up to about 9 the influence of III is relatively unimportant. Since the plot made from the measurements at 18.0×10^3 cm^{-1} seems to fit with a straight line all the way up to the formality ratio 7, there is very little $TeCl_3^+$ present after this formality ratio. In the range from about 9 to about 13.5, the plots made for both wavenumbers give curved lines indicating more than two species (i.e., Te_4^{2+}, II, and III).

As in the work on the low oxidation states of selenium[13] we decided to treat the data in all formality ranges with model reactions of the form

$$h\mathrm{Te}_q^{r+} + j\mathrm{Te}_y^{z+} \rightleftarrows k\mathrm{Te}_v^{x+} \qquad (16)$$

where h, j, and k are integers. The limitation for the models was as in the spectrophotometric work on the oxidation states of selenium[13] that charges higher than 4+ are not considered. A survey of the chemical literature shows that few compounds have a positive charge higher than 4+. In the formality ratio range 0.30–9.18 Te_q^{r+} will then have to represent Te^{4+} (in the form of $TeCl_3^+$) and Te_y^{z+} and Te_v^{x+} will have to represent II and I, respectively. Since both Corbett and co-workers[3] and Gillespie and co-workers[5] have found tellurium in the oxidation state $+^1/_3$ and since a charge of 2+ seems the most reasonable (in order to get diamagnetic species the charge will have to be either 2+ or 4+, and 4+ seems a rather high charge), Te_6^{2+} was chosen as the most reasonable formula for II. The values of v and x in the formula for I (i.e., Te_v^{x+}) were changed systematically in such a way that the oxidation state of I (i.e., x/v) was close to $+^1/_2$ (the sharp break in Figure 3 corresponds to an oxidation state of $+^1/_2$). By using the method outlined in the Methods of Investigation the minimum variances for all of the different model reactions could be cal-

Table I. Variances Based on Spectrophotometric Measurements for Models[a] with Oxidation States Close to $+^1/_2$[b]

Oxidn state	Formal charge 1+	2+	3+	4+
$+^2/_3$		1.3×10^{-3}		1.1×10^{-3}
$+^3/_5$			6.0×10^{-4}	
$+^4/_7$				7.0×10^{-4}
$+^1/_2$	1.8×10^{-5}*	1.8×10^{-5}*	2.7×10^{-5}*	1.9×10^{-5}*
$+^4/_9$				2.3×10^{-3}
$+^3/_7$			5.2×10^{-4}	
$+^2/_5$		1.7×10^{-1}		1.5×10^{-3}

[a] Other species in the equilibria assumed to be Te^{4+} and Te_6^{2+}. [b] Number of spectra 10; number of different wavenumbers 121; wavenumber range 8.3×10^3–30.8×10^3 cm^{-1}; formality ratio range 0.29_7–9.18_3; asterisks based on $F_{0.10}(7, 7) = 2.78$.

Table II. Variances Based on Spectrophotometric Measurements for Models[a] with Oxidation States Close to $+^1/_3$[b]

Oxidn state	Formal charge 1+	2+	3+	4+
$+^3/_7$			2.4×10^{-4}	
$+^2/_5$		3.4×10^{-4}		1.8×10^{-4}
$+^3/_8$			9.8×10^{-5}*	
$+^4/_{11}$				1.5×10^{-4}*
$+^1/_3$	2.8×10^{-5}*	2.7×10^{-5}*	1.3×10^{-4}*	1.3×10^{-4}*
$+^4/_{13}$				6.8×10^{-4}
$+^3/_{10}$			6.1×10^{-4}	
$+^2/_7$		3.1×10^{-4}		7.0×10^{-4}

[a] Other species in the equilibria assumed to be Te_4^{2+} and Te_8^{2+}. [b] Number of spectra 6; number of different wavenumbers 121; wavenumber range 8.3×10^3–30.8×10^3 cm^{-1}; formality ratio range 7.48_9–13.59_1; asterisks based on $F_{0.10}(3, 3) = 5.39$.

culated. The results of these calculations are shown in Table I. To distinguish as well as possible between the different models a smoothing procedure was applied to the measured spectra used in this table and in other tables. In this procedure the absorbance of the middle point of three successive points was obtained by a linear least-squares interpolation.[20] The equilibrium constants have not been given in Table I in order to save space. As mentioned above Te_6^{2+} was chosen in the model reactions to represent II. However, other formulations of II with oxidation states close to $+^1/_3$ will not change the general picture of the calculations shown in Table I.

From the variance in Table I (calculated with respect to the deviations between the measured and calculated absorbances at all wavenumbers) it is clear that the species with oxidation states $+^1/_2$ give better fit than any of the other species. In order to distinguish between the models we applied an F test[21] to the results with the lowest obtained variance as the denominator and based the distinction on 10% probability points. Under these circumstances the species with oxidation state $+^1/_2$ was found to give a significantly better fit than any of the other oxidation states and was therefore marked with asterisks. To obtain the value of $F\alpha$ (ϕ_N, ϕ_D) (where α is the probability point and ϕ_N and ϕ_D are the numbers of degrees of freedom in the nominator and denominator, respectively) it was assumed that ϕ_N and ϕ_D were equal to the number of different melt compositions minus 3. The reason for looking only at melt compositions and not at total numbers of measured absorbances (as has been done in order to get the variances shown in Table I) was that these absorbances were not truly independent of each other, since they belonged in groups to particular formality ratios.

In Table II are shown the results of similar calculations for the formality ratio range 7.49–13.59. In these calculations the formulations Te_4^{2+} and Te_8^{2+} have been used for species I and III, respectively, but other formulations of these species with oxidation states close to $+^1/_2$ and $+^1/_4$ will not change the general picture of the calculations shown in Table II. From Table II it is clear that two of the four species with oxidation state $+^1/_3$ give better fit than any of the other species. If we apply an F test (based on 10% probability points) to the results in Table II, possible formulas for species II (marked with asterisks) are Te_{3n}^{n+} (n = 1–4), Te_8^{3+}, and Te_{11}^{4+}. In Table III is shown the result of calculations in the same formality range as in Table II. The asterisks indicate as before models within 90% probability of the best model. The formulas Te_4^{2+} and Te_6^{2+} have here been used for species I and II, respectively. As can be seen from Table III it is not possible based on 10% probability points to distinguish between the different shown species.

Table III. Variances Based on Spectrophotometric Measurements for Models[a] with Oxidation States Close to $+^1/_4$[b]

Oxidn state	Formal charge 1+	2+	3+	4+
$+^4/_{15}$				2.7×10^{-5}*
$+^1/_4$	1.3×10^{-4}*	2.7×10^{-5}*	3.1×10^{-5}*	4.4×10^{-5}*
$+^4/_{17}$				6.1×10^{-5}*
$+^3/_{13}$			5.0×10^{-5}*	
$+^2/_9$		3.7×10^{-5}*		7.4×10^{-5}*

[a] Other species in equilibria assumed to be Te_4^{2+} and Te_6^{2+}. [b] Number of spectra 6; number of different wavenumbers 121; wavenumber range 8.3×10^3–30.8×10^3 cm^{-1}; formality ratio range 7.48_9–13.59_1; asterisks based on $F_{0.10}(3, 3) = 5.39$.

Potentiometric Study of Tellurium Species Formed in the NaCl–$AlCl_3$ (37:63 mol %) Melt. The potential of the used electrochemical cell can as shown in Methods of Investigation be given by eq 15. If we look at the formality ratio range 0.01–6.97 and assume that the tellurium species present are $TeCl_3^+$, Te_4^{2+}, and Te_6^{2+} and that the ionic radii for Na^+, $Al_2Cl_7^-$, $AlCl_4^-$, $TeCl_3^+$, Te_4^{2+}, and Te_6^{2+} are 1.0, 5.1, 3.3, 3.2, 2.6, and 3.3 Å, respectively, the sum of the last six terms in eq 14 can be calculated to obtain a maximum value of 0.14 mV (the individual values are +0.22, −0.03, −0.02, +0.20, −0.23, and −0.00 mV, respectively). This calculation is based on a formality ratio and formal concentration of $TeCl_4$ in compartment I of 3.00 and 0.092 and in compartment II of 6.97 and 0.092, respectively. The concentrations of $Al_2Cl_7^-$ and $AlCl_4^-$ were obtained from the work of Boxall, Jones, and Osteryoung.[12] The sum of the last six terms in eq 15 is small compared to the maximum $|\Delta E|$ obtainable in these systems and are therefore neglected. A similar calculation for the formality range 9.00–14.4 showed that also in this case the six last terms could be neglected. Within the experimental uncertainty the potential of the used concentration cell can now be given as

$$\Delta E = \frac{RT \ln 10}{F} \log \frac{[Te_q^{r+}]_{II}^{n^{-1}v} [Te_v^{x+}]_I^{n^{-1}q}}{[Te_q^{r+}]_I^{n^{-1}v} [Te_v^{x+}]_{II}^{n^{-1}q}} \qquad (17)$$

where $[Te_q^{r+}]_I$, $[Te_v^{x+}]_I$ and $[Te_q^{r+}]_{II}$, $[Te_v^{x+}]_{II}$ are the concentrations in cell compartments I and II, respectively.

To avoid a large difference in concentrations of solute species in the two cell compartments the composition in the compartments was increased alternately, while interchanging the compartments used for measurement and reference. A small difference in composition between the two cell compartments will reduce the possibility of vapor transport of material from one chamber to the other. In the measurements given in Table IV all ΔE values refer to the original reference compositions called the basic reference melts. A plot of the measured ΔE versus the Te:$TeCl_4$ formality ratio is given in Figure 4. This plot shows some of the same features as the spectrophotometric plot (Figure 3). It is for example clear that there must be a radical change in concentrations of the species around a formality ratio of 7. It is important to notice that there is no

Table IV. Values of Cell Potential at Different Formalities of Te and $TeCl_4$ in Molten NaCl-$AlCl_3$ (37:63 mol %)[a] at 150 °C

ΔE, mV	c'_{Te} (formality of Te)	$c'_{Te(IV)}$ (formality of $TeCl_4$)	R (Te:$TeCl_4$ formality ratio)
21.7_8[c]	0.01_1	0.0921_9	0.01_2
20.4_1[b]	0.001_3	0.0923_7	0.01_4
16.9_0[b]	0.004_2	0.0923_6	0.04_6
11.6_8[c]	0.046_9	0.0921_0	0.50_9
0.5_9[c]	0.273_3	0.0916_8	2.98_1
-3.1_4[b]	0.365_3	0.0920_0	3.97_1
-9.3_2[b]	0.454_7	0.0918_3	4.95_1
-17.0_2[b]	0.546_2	0.0916_6	5.95_9
-24.5_0[c]	0.587_5	0.0910_8	6.45_1
-41.4_8[b]	0.638_0	0.0914_8	6.97_4
-72.3_5[c]	0.641_5	0.0909_9	7.05_1
-84.8_2[c]	0.651_0	0.0909_6	7.15_7
-130.3_9[c]	0.671_6	0.0909_3	7.38_6
-159.5_4[c]	0.712_9	0.0908_4	7.84_7
-161.3_5[b]	0.727_8	0.0913_1	7.97_1
-208.0_9[c]	0.815_8	0.0906_6	8.99_9
-238.1_7[b]	0.908_8	0.0909_7	9.99_0
-259.6_5[c]	0.950_4	0.0904_0	10.51_3
-274.7_9[c]	0.995_2	0.0903_2	11.01_8
-287.4_9[c]	1.028_7	0.0902_6	11.39_8
-308.7_7[b]	1.087_6	0.0906_4	12.00_0
-362.0_7[c]	1.176_0	0.0899_8	13.06_9
-377.9_7[b]	1.267_4	0.0903_0	14.03_6
-383.4_2[c]	1.345_5	0.0896_6	15.00_6
-381.0_0[c]	1.364_3	0.0896_6	15.21_6

[a] In each cell compartment was ca. 10.30 g of NaCl-$AlCl_3$ melt. [b] Potentiometric cell no. 1. Composition of basic reference melt: $R = 2.99_8$, $c'_{Te(IV)} = 0.0921_7$. [c] Potentiometric cell no. 2. Composition of basic reference melt: $R = 2.99_0$, $c'_{Te(IV)} = 0.0916_7$.

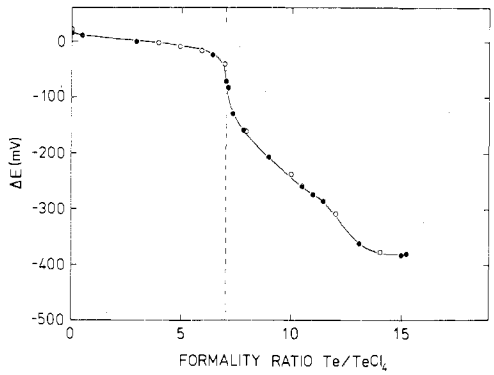

Figure 4. Measured ΔE values as a function of the Te:$TeCl_4$ formality ratio. Values were taken from Table IV: open circles, cell no. 1; filled circles, cell no. 2. Dashed line indicates formality ratio 7.

change in composition after a formality of ca. 15 is reached.

We decided first to look at the formality ratio range in which only two species were present (i.e., the ranges in which straight lines are obtained in Figure 3). If only two species are present, the concentrations of the two chosen models (Te_q^{r+} and Te_v^{x+}) can be calculated from the formality ratio Te:$TeCl_4$ and the formal concentration of $TeCl_4$. If the correct formulas of Te_q^{r+} and Te_v^{x+} are used for the species in cell compartment II and the measured ΔE values are plotted vs. log $[Te_q^{r+}]_{II}^{n^{-1}v}/[Te_v^{x+}]_{II}^{n^{-1}q}$, one should obtain a straight line with the slope $RT \ln 10/F$. A plot of this type is shown for the formality ratio range 0.01–5.96 in Figure 5. Since Te_q^{r+} has a higher oxidation state than Te_v^{x+}, they are designated Ox and Red, respectively. The basic reference with formality ratio of 2.99_8 and formal concentration of $TeCl_4$ of 0.0921_7 is here used as solution I. We have in agreement with Table I assumed that the oxidation state of Te_v^{x+} is $+^1/_2$ (the formula for Te_q^{r+} is of course Te^{4+}) and have made calculations for all of the

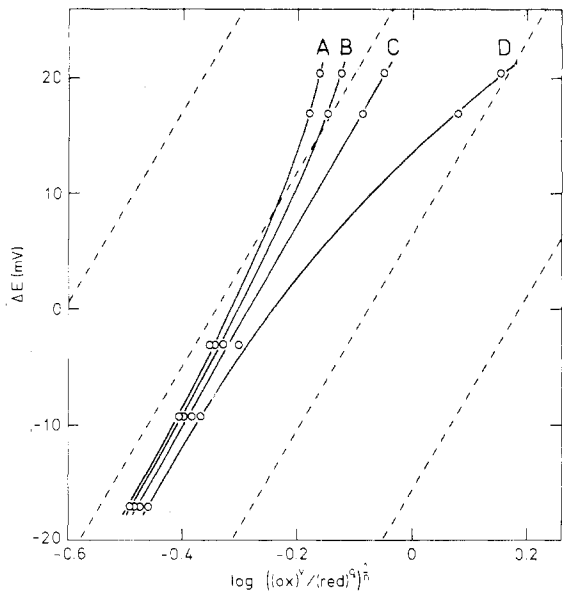

Figure 5. Relation between the measured ΔE taken from Table IV and the calculated value of log $((Ox)^v/(Red)^q)^{1/n}$ for the formality ratio range 0.001_3–0.546_2. Formulas for Ox and Red and values of v, q, and n: A, Te^{4+}, Te_8^{4+}, 8, 1, 28; B, Te^{4+}, Te_6^{3+}, 6, 1, 21; C, Te^{4+}, Te_4^{2+}, 4, 1, 14; D, Te^{4+}, Te_2^{+}, 2, 1, 7. The dashed lines give the theoretical slope. Measurements were made with cell no. 1.

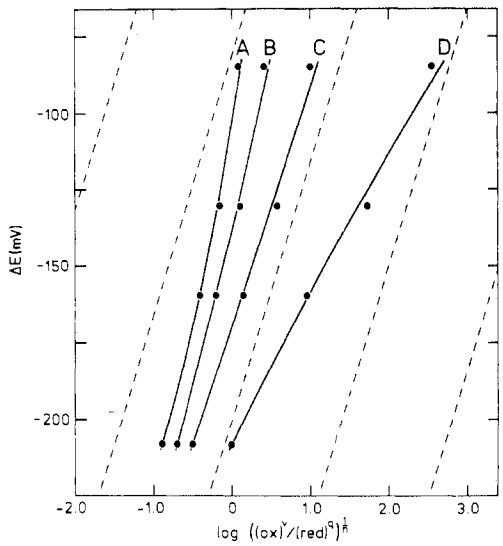

Figure 6. Relation between the measured ΔE taken from Table IV and the calculated value of log $((Ox)^v/(Red)^q)^{1/n}$ for the formality ratio range 7.15_7–8.99_9. Formulas for Ox and Red and values of v, q, and n: A, Te_4^{2+}, Te_{12}^{4+}, 3, 1, 2; B, Te_4^{2+}, Te_9^{3+}, 9, 4, 6; C, Te_4^{2+}, Te_6^{2+}, 3, 2, 2; D, Te_4^{2+}, Te_3^{+}, 3, 4, 2. The dashed lines give the theoretical slope. Measurements were made with cell no. 2.

possible species with oxidation state $+^1/_2$. From this plot it is clear that a formulation of Te_v^{x+} of Te_4^{2+} gives a better fit than any of the other species. The existence of Te_4^{2+} is in agreement with previous work.[1] A similar plot can be made for the formality ratio range 7.16–9.00, where according to the spectrophotometric work a species with oxidation state $+^1/_2$ (i.e., Te_4^{2+}) should be present besides a species with oxidation state $+^1/_3$. As can be seen from the plot in Figure 6 again one of the models gives an almost straight line, which has a slope fairly close to the theoretical value. This line is calculated with Te_4^{2+} as Ox and Te_6^{2+} as Red.

Since there is no two-species range in which the last species (i.e., III) takes part, it is obvious that the described method

Table V. Variances Based on Potentiometric Measurements for Models[a] with Oxidation States Close to $+^1/_2$[b]

Oxidn state	Formal charge 1+	2+	3+	4+
$+^2/_3$		(1.3×10^4)		(4.4×10^3)
$+^3/_5$			$(2.2 \times 10^{3*})$	
$+^4/_7$				(3.7×10^3)
$+^1/_2$	3.5×10^3	$1.1 \times 10^{3*}$	(3.7×10^3)	4.9×10^3
$+^4/_9$				(5.5×10^3)
$+^3/_7$			(6.2×10^3)	
$+^2/_5$		4.4×10^3		5.9×10^3

[a] Other species in the equilibria assumed to be Te^{4+} and Te_6^{2+}. [b] Number of measurements 10; formality ratio range 0.01_2–6.97_4; asterisks based on $F_{0.10}(9, 9) = 2.44$. Parentheses indicate that no minima were found; the values given are then for equilibrium constants of either 10^{+60} or 10^{-60}.

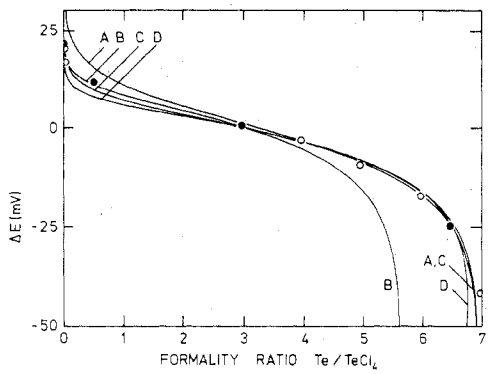

Figure 7. Measured ΔE values taken from Table IV (open circles, cell no. 1; filled circles, cell no. 2) as a function of the Te:$TeCl_4$ formality ratio compared with values (full lines) calculated from the weighted experimental data for the four reaction schemes with the lowest variances in Table V. Species in equilibrium with Te^{4+} and Te_6^{2+}: A, Te_2^+; B, Te_5^{3+}; C, Te_4^{2+}; D, Te_6^{3+}.

cannot be used for this case. A more general way is to start with the mass action relation associated with eq 16 and, as in the case of the spectrophotometric calculations, start for each model equation with an arbitrarily chosen equilibrium constant, calculate the concentration of each species, and introduce the calculated concentrations in eq 17. By varying systematically the equilibrium constant for the particular model equilibrium we are considering, it is possible to minimize the deviation (least squares) between the formality ratios calculated from ΔE and the formality ratios directly calculated from the weighings. As before the limitation for the models was that charges higher than 4+ were not considered. In the calculation shown in Table V the basic reference melt is solution I. The parentheses around some of the variances in this table (and in similar tables) indicate that no minimum was found in such cases. The values given are here calculated from equilibrium constants of either 10^{+60} or 10^{-60}. Since the variances varied very little with respect to the equilibrium constants at these extreme values, the given variances are assumed to be correct. The models in Table V marked with asterisks indicate as before that the variances for these models are within the 90% probability range of the lowest obtained variance. As can be seen from Table V the potentiometric method seems to be more selective than the spectrophotometric method. What is important is that if the two methods are combined, only one species (Te_4^{2+}) will fit both methods. A graphical comparison of the four models with the lowest variance (see Table V) is shown in Figure 7. From this figure it can be seen that only curve C (corresponding to formation of Te_4^{2+}) fits well at both high and low formality ratios. Curve B which corresponds with formation of Te_5^{3+} fits rather poorly at high formality ratios, but according to Table V it is the next best model. This is because the sum of squares for each model has been weighted by the inverse of the associated variance for each formality ratio.[21] The same weighting procedure has been used for all potentiometric calculations in which the mass action equation associated with eq 16 has been used. The associated variance for each formality ratio is calculated from an estimated average error of ±0.14 mg in the weight of tellurium and of ±0.40 mg in the weight of $TeCl_4$. It is more difficult to obtain the correct weight for the powdery $TeCl_4$ than for the more metallic and heavier tellurium, since $TeCl_4$ is more liable to stick to the surface of the funnels used to fill the electrode cells. The influence of this weighting of the data is only of importance for the calculations on the measurements in formality ratio range from 0 to 7. Since the melt in itself is slightly reducing, all formal concentrations of tellurium were corrected by adding 0.03 mg of tellurium to the weight of tellurium and by subtracting 0.06 mg of $TeCl_4$ from the weight of $TeCl_4$ added. These amounts of tellurium and $TeCl_4$ were found by measuring the potential of "pure" $TeCl_4$ against one of the basic references and recognizing that Te_4^{2+} was formed by the reduction of Te(IV).

Table VI. Variances Based on Potentiometric Measurements for Models[a] with Oxidation States Close to $+^1/_3$[b]

Oxidn state	Formal charge 1+	2+	3+	4+
$+^3/_8$			(7.3×10^3)	
$+^4/_{11}$				(5.5×10^3)
$+^1/_3$	1.0×10^2	$3.0 \times 10^*$	(2.3×10^3)	$7.9 \times 10^*$
$+^4/_{13}$				(1.1×10^3)
$+^3/_{10}$			9.9×10^2	

[a] Other species in the equilibria assumed to be Te_4^{2+} and Te_8^{2+}. [b] Number of measurements 8; formality ratio range 8.99_9–14.03_6; asterisks based on $F_{0.10}(7, 7) = 2.78$. Parentheses indicate that no minima were found; the values given are then for equilibrium constants of either 10^{+60} or 10^{-60}.

In Table VI are similarily given the variances for models with oxidation states close to $+^1/_3$; the other species in the equilibrium (besides Te_4^{2+}) is assumed to be Te_8^{2+} just as in the case of the spectrophotometric measurements. The compositions with formality ratios of 7.97_1 or 7.84_7 and formal concentrations of $TeCl_4$ of 0.0913_1 or 0.0908_4 for potentiometric cells no. 1 or no. 2, respectively, have here been used to represent solution I. As can be seen from Table VI only two models seem to give reasonable fits (i.e., Te_6^{2+} and Te_{12}^{4+}). Unfortunately, a comparison with the similar calculations for the spectrophotometric measurements (Table II) will not exclude any of these species. From Table VI it can be shown, however, that if we, instead of 10% probability points, work with 12.5% probability points, only Te_6^{2+} will be included within the 87.5% probability. It should be noted that working with 12.5% probability points will also exclude Te_{12}^{4+} in the spectrophotometric work (Table II). On the basis of this Te_6^{2+} seems to be the correct formula for species II. In Figure 8 is shown a graphical comparison among the four models with the lowest variances in Table VI. We know now that two of the species in the three-species region are Te_4^{2+} and Te_6^{2+}. In Table VII are shown calculations where the oxidation state of the third species is varied around a value of $+^1/_4$. These calculations are based on the same measurements as the calculations in Table VI. In Figure 9 is given a graphical comparison among the four models with the lowest variances in Table VII. From calculations given in Table VII it can be seen that only two models (Te_4^+ and Te_8^{2+}) give reasonable fits. Comparison with similar calculations from the spectrophotometric work will as before not exclude any of these species. However, if we work with 12.5% probability points Te_4^+ will be excluded both in the potentiometric and in the spectrophotometric measurements. On the basis of this

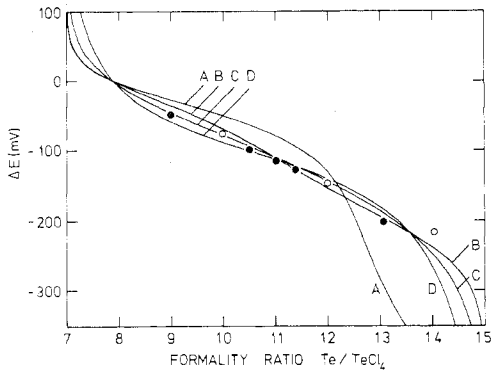

Figure 8. Measured ΔE values (open circles, cell no. 1; filled circles, cell no. 2) as a function of the formality ratio compared with values (full lines) calculated from the weighted experimental data for the four reaction schemes with the lowest variances in Table VI. Composition of reference melts: Te:$TeCl_4$ formality ratio 7.97_1 or 7.84_7 and formality of $TeCl_4$ 0.0913_1 or 0.0908_4, for cell no. 1 or 2, respectively. Species in equilibrium with Te_4^{2+} and Te_8^{2+}: A, Te_{10}^{3+}; B, Te_{12}^{4+}; C, Te_6^{2+}; D, Te_3^{+}.

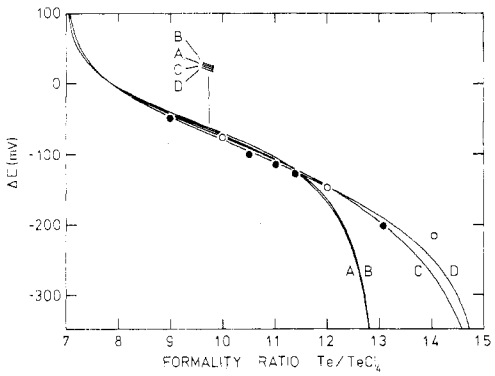

Figure 9. Measured ΔE (open circles, cell no. 1; filled circles, cell no. 2) as a function of the formality ratio compared with values (full lines) calculated from the weighted experimental data for the four reaction schemes with the lowest variances in Table VII. Composition of reference melts: Te:$TeCl_4$ formality ratio 7.97_1 or 7.84_7 and formality of $TeCl_4$ 0.0913_1 or 0.0908_4, for cell no. 1 or 2, respectively. Species in equilibrium with Te_4^{2+} and Te_6^{2+}: A, Te_{14}^{4+}; B, Te_7^{2+}; C, Te_4^{+}; D, Te_8^{2+}.

Table VII. Variances Based on Potentiometric Measurements for Models[a] with Oxidation States Close to $+^1/_4$[b]

Oxidn states	Formal charge			
	1+	2+	3+	4+
$+^2/_7$		4.2×10^2		4.1×10^2
$+^3/_{11}$			(2.6×10^3)	
$+^4/_{15}$				(2.6×10^3)
$+^1/_4$	$7.6 \times 10^*$	$3.0 \times 10^*$	(2.6×10^3)	(2.6×10^3)
$+^4/_{17}$				(2.6×10^3)
$+^3/_{13}$			(2.6×10^3)	
$+^2/_9$		(2.6×10^3)		(2.6×10^3)
$+^3/_{14}$			(2.6×10^3)	

[a] Other species in the equilibria assumed to be Te_4^{2+} and Te_6^{2+}. [b] Number of measurements 8; formality ratio range 8.99_9–14.03_6; asterisks based on $F_{0.10}(7, 7) = 2.78$. Parentheses indicate that no minima were found; the values given are then for equilibrium constants of either 10^{+60} or 10^{-60}.

Te_8^{2+} seems to be the correct formula for III.

The calculated spectra of the four tellurium species, Te^{4+} (as $TeCl_3^+$), Te_4^{2+}, Te_6^{2+}, and Te_8^{2+}, are given in Figure 10. In Table VIII are given the equilibrium constants for the reactions $2Te^{4+}(soln) + 7Te_6^{2+}(soln) \rightleftarrows 11Te_4^{2+}(soln)$ and $Te_4^{2+}(soln) + Te_8^{2+}(soln) \rightleftarrows 2Te_6^{2+}(soln)$. From this table it is clear that the pK value for the second shown reaction is much better determined than the pK value for the first shown

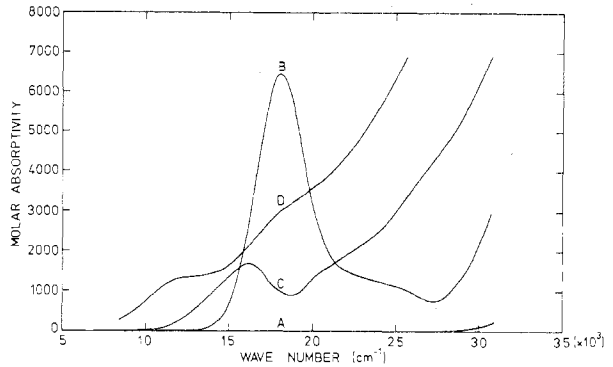

Figure 10. Calculated spectra of (A) Te^{4+} (probably as $TeCl_3^+$), (B) Te_4^{2+}, (C) Te_6^{2+}, and (D) Te_8^{2+}. The spectra of Te^{4+} and Te_4^{2+} were calculated on the basis of ten measured spectra, whereas the spectra of Te_6^{2+} and Te_8^{2+} were calculated on the basis of six measured spectra.

Table VIII. pK Values[a] for the Equilibria $2Te^{4+}(soln) + 7Te_6^{2+}(soln) \rightleftarrows 11Te_4^{2+}(soln)$ (1) and $Te_4^{2+}(soln) + Te_8^{2+}(soln) \rightleftarrows 2Te_6^{2+}(soln)$ (2) in Molten $NaCl$-$AlCl_3$ (37:63 mol %)

Method	pK_1	Confidence limits for pK_1 (95%)	pK_2	Confidence limits for pK_2 (95%)
Spectrophotometric, 250 °C	−12	−∞ to −9	−0.4	−0.2 to −2.2
Potentiometric, 150 °C	−17	−∞ to −10	−0.93	−1.03 to −0.84

[a] Based on molar concentrations.

reaction. Unfortunately, it is not possible to compare the two methods directly, since they are performed at different temperatures. However, there seems to be no contradiction between the two methods, especially if the temperature difference is taken into consideration. Since we have obtained the equilibrium constants, we are now able to check the two-species ranges at 150 °C found from the straight lines in Figure 3 at 250 °C. In the range from 0 to 7 it is clear that we have close to a two-species system. At the lowest formality ratio in this range (0.01_2) the percentages of Te(IV) and Te_4^{2+} are approximately 99.8% and 0.2%, whereas the concentrations of Te_6^{2+} and Te_8^{2+} are 10^{-5}% and 10^{-11}%, respectively. At the highest formality ratio in this range (6.97_4) the percentages of Te(IV), Te_4^{2+}, Te_6^{2+}, and Te_8^{2+} are approximately 0.7%, 99.0%, 0.3%, and 10^{-4}%, respectively. In the range from 7 to 9 there is likewise a two-species system. This can be seen from the following percentages. At the lowest measured formality ratio in this range (7.05_1) the percentages of Te(IV), Te_4^{2+}, Te_6^{2+}, and Te_8^{2+} are approximately 0.2%, 98.5%, 1.3%, and 10^{-3}%, respectively. At the highest measured formality in this range (8.99_9), the percentages of Te(IV), Te_4^{2+}, Te_6^{2+}, and Te_8^{2+} are approximately 10^{-8}%, 53.9%, 42.3%, and 3.9%, respectively.

Acknowledgment. The authors wish to thank B. Lottrup Knudsen for help with programming and to acknowledge the financial support of Statens teknisk-videnskabelige Forskningsrad.

Registry No. Te_4^{2+}, 12597-50-1; Te_6^{2+}, 39448-81-2; Te_8^{2+}, 59588-10-2; $TeCl_4$, 10026-07-0; Te, 13494-80-9.

References and Notes

(1) N. J. Bjerrum, *Inorg. Chem.*, **9**, 1965 (1970).
(2) N. J. Bjerrum, *Inorg. Chem.*, **10**, 2578 (1971).
(3) D. J. Prince, J. D. Corbett, and B. Garbisch, *Inorg. Chem.*, **9**, 2731 (1970).
(4) T. W. Couch, D. A. Lokken, and J. D. Corbett, *Inorg. Chem.*, **11**, 357 (1972).
(5) J. Barr, R. J. Gillespie, G. P. Pez, P. K. Ummat, and O. C. Vaidya, *Inorg. Chem.*, **10**, 362 (1971).
(6) N. J. Bjerrum, *Inorg. Chem.*, **11**, 2648 (1972).
(7) J. H. von Barner and N. J. Bjerrum, *Inorg. Chem.*, **12**, 1891 (1973).

(8) H. A. Andreasen and N. J. Bjerrum, *Inorg. Chem.*, **14**, 1807 (1975).
(9) A. Damiens, *Ann. Chim. (Paris)*, **18**, 282 (1922).
(10) J. H. Simons, *J. Am. Chem. Soc.*, **52**, 3488 (1930).
(11) C. R. Boston, *J. Chem. Eng. Data*, **11**, 262 (1966).
(12) L. G. Boxall, H. L. Jones, and R. A. Osteryoung, *J. Electrochem. Soc.*, **120**, 223 (1973).
(13) R. Fehrmann, N. J. Bjerrum, and H. A. Andreasen, *Inorg. Chem.*, **14**, 2259 (1975).
(14) J. H. von Barner, N. J. Bjerrum, and K. Kiens, *Inorg. Chem.*, **13**, 1708 (1974).
(15) E. A. Guggenheim, "Thermodynamics", North-Holland Publishing Co., Amsterdam, 1967, pp 321–324.
(16) H. S. Harned and B. B. Owen, "The Physical Chemistry of Electrolytic Solutions", 3d ed, Reinhold, New York, N.Y., 1958, p 231.
(17) G. J. Janz, Ed., "Molten Salts Handbook", Academic Press, New York, N.Y. 1967, pp 344–345.
(18) P. Brekke, J. H. von Barner, and N. J. Bjerrum, to be submitted for publication.
(19) F. W. Poulsen, N. J. Bjerrum, and O. F. Nielsen, *Inorg. Chem.*, **13**, 2693 (1974).
(20) IBM Application Program, System 1360 Scientific Subroutine Package, Version III, SE 13.
(21) See for example O. L. Davies and P. L. Goldsmith, "Statistical Methods in Research and Production", Oliver and Boyd, Edinburgh, 1972.

Contribution from the Institute of Scientific and Industrial Research, Osaka University, Suita, Osaka 565, Japan

Synthesis and Some Properties of $FeOOCH_3$. A New Layered Compound

SHINICHI KIKKAWA, FUMIKAZU KANAMARU, and MITSUE KOIZUMI*

Received February 3, 1976 AIC600877

A new layered compound was synthesized by soaking an intercalated compound $FeOCl(4\text{-}AP)_{1/4}$ in methanol at 110 °C for 6 days. This new compound had a chemical composition of $FeOOCH_3$ and its interlayer spacing was 9.97 Å. The infrared spectrum showed two kinds of absorption bands of C–O stretching vibration around 1050 cm^{-1}, but no O–H stretching vibration. A study of the Mössbauer effect of $FeOOCH_3$ at room temperature indicated that the isomer shift and the quadrupole splitting were 0.37 and 0.60 mm/s, respectively. The crystal structure is characterized by a layer structure derived from FeOCl or γ-FeOOH.

Introduction

Many organic intercalation complexes of layered compounds have been prepared and characterized. Among them, clay–organic complexes have been extensively investigated in the field of earth science, agriculture, and crystal chemistry.[1,2] In recent years, many investigations have been done on the complexes of layered inorganic compounds and organic molecules, for example, $TaS_2(py)_{1/n}$, from the viewpoint of material science.[3] In these complexes the intercalated organic molecules are loosely bonded to the layer surface of the host inorganic material. Kanamaru et al. have reported the synthesis and properties of this type of complex of FeOCl and pyridine.[4] On the other hand, few compounds of the directly bonded type have been reported, that is to say organic derivatives in which the layered structure is retained.[5] We succeeded in the preparation of the latter type compound $FeOOCH_3$ by replacing Cl of FeOCl with OCH_3. This paper describes the preparation and some properties of the $FeOOCH_3$.

Experimental Section

Preparation. FeOCl was prepared by heating the mixture of α-Fe_2O_3 and $FeCl_3$ with the mole ratio of 1 to $^4/_3$ in a sealed Pyrex glass tube at 370 °C for 2 days. Reddish violet and thin blade-like FeOCl crystals with dimensions 10 × 2 × 0.5 mm were obtained. To remove excess $FeCl_3$, the product was washed with water and dried. Then FeOCl was reacted with acetone solution of 4-aminopyridine (4-AP) at 110 °C for 6 days in a sealed glass tube. Black crystals of the intercalation compound of 4-AP and FeOCl were obtained. This compound was soaked in methanol in a sealed Pyrex glass tube. The duration of the reaction which produced brown crystals of $FeOOCH_3$ was about 10 days at 80 °C but 6 days at 110 °C.

Analysis. X-ray analysis was conducted with a Rigaku-Denki diffractometer using Cu Kα and Co Kα radiation. A C, H, N, and Cl analysis of this complex was made using standard techniques. Infrared absorption spectra were obtained using a Japan Spectroscopic Co. Ltd. DS-402G spectrometer by the usual KBr pellet technique and Nujol method. Mössbauer spectra using radiation from ^{57}Co in Cu metal were measured at room temperature with a 200 channel multichannel analyzer. Calibration was based on the Mössbauer spectrum of Fe metal. For differential thermal analysis a Rigaku-Denki apparatus fitted with a platinum platinum–rhodium thermocouple was used and Al_2O_3 was used as reference. The rate of temperature increase was 10 °C/min.

Table I. X-Ray Powder Diffraction Data for $FeOOCH_3$[a,b]

hkl	I	d_{obsd}	d_{calcd}
010	vs	9.91	9.97
020	m	4.99	4.98
001	w	3.99	3.99
110	mm	3.58	3.58
030	mm	3.33	3.32
120	w	3.03	3.04
040	w	2.491	2.492
002	vw	2.003	1.995
050	mm	1.992	1.994
200	w	1.921	1.915
060	mm	1.662	1.662
070	vw	1.426	1.425

[a] Debye–Scherrer data; Co Kα radiation. [b] $a = 3.83$ (1) A, $b = 9.97$ (1) A, $c = 3.99$ (1) A.

Results and Discussion

Due to a strong preferred orientation effect, each x-ray diffraction pattern presented in Figure 1 consists of only basal reflection lines of each product obtained in the above-mentioned reaction process. FeOCl belongs to the orthorhombic space group *Pmnm* with $a = 3.780$, $b = 7.917$, $c = 3.302$ Å, and $Z = 2$.[6] The crystal structure is characterized by the layer structure similar to that of γ-FeOOH. The layer consists of a double sheet of *cis*-$FeCl_2O_4$ octahedra linked together by shared edges through oxygens. The outermost atoms on each side of the layers are Cl^- ions. The interlayer force between adjacent layers is weak van der Waals'. When FeOCl was heated with acetone solution of 4-AP, 4-AP molecules could penetrate into the van der Waals gap, and then the sorption complex $FeOCl(4\text{-}AP)_{1/4}$ was obtained.[7] This reaction was accompanied by the expansion of FeOCl lattice along the *b* axis to give the basal spacing of 13.57 Å as shown in Figure 1b. One-dimensional electron-density projection on the *b* axis of $FeOCl(4\text{-}AP)_{1/4}$ was synthesized using the eight (0*k*0) reflections. The schematic structure based on the projection is illustrated in Figure 2b. During the reaction of the sorption complex $FeOCl(4\text{-}AP)_{1/4}$ and methanol, methanol molecules were easily intercalated in the expanded interlayer spaces of FeOCl, and the third phase appeared. The last phase gave the basal spacing of 9.97 Å as depicted in Figure 1c and Table